

Supporting information

Stable Color-Tunable $\text{Ca}_3\text{Y}(\text{GaO})_3(\text{BO}_3)_4$: $\text{Bi}^{3+}/\text{Tb}^{3+}/\text{Eu}^{3+}$ Phosphors for Application in n -UV Pumped w LEDs

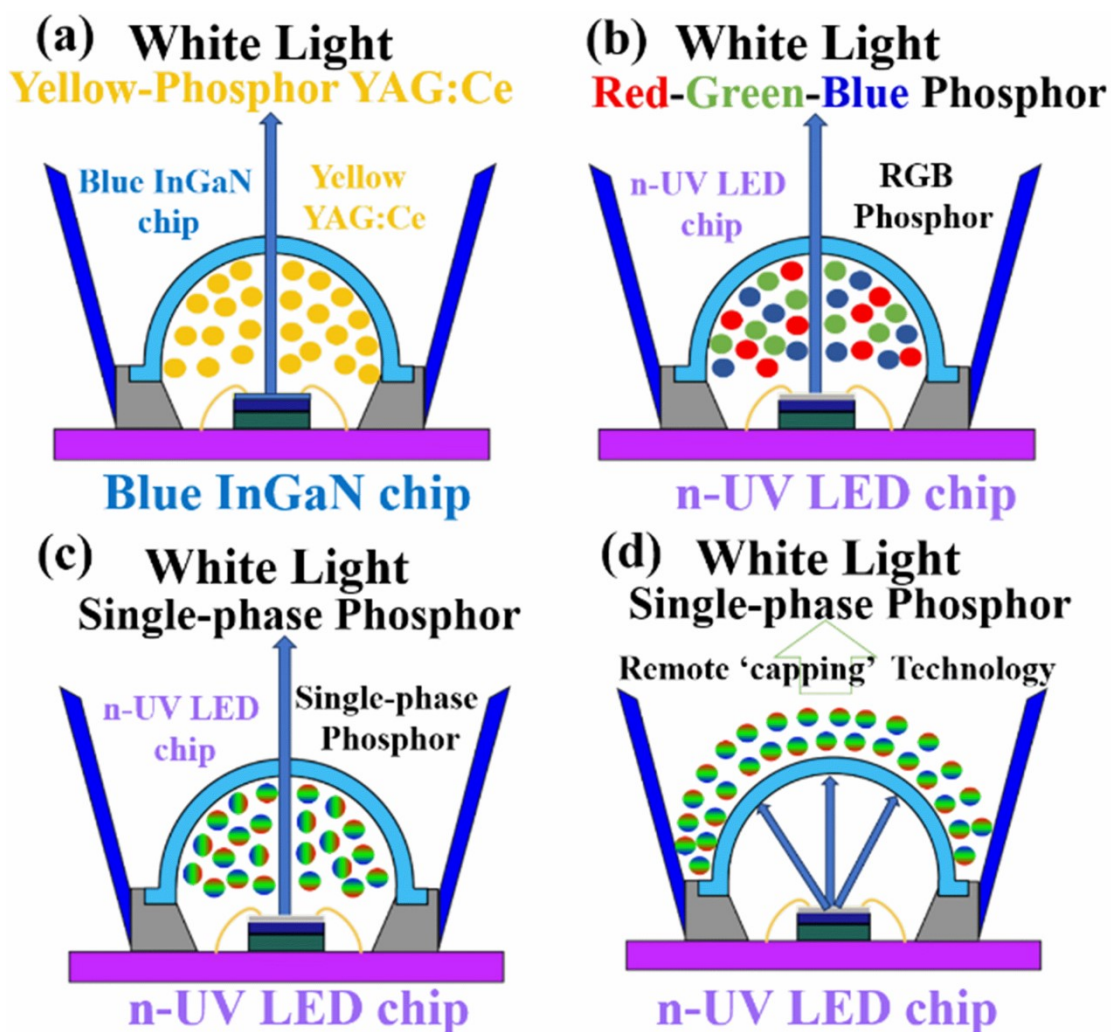
*P. J. Xia¹, X. Z. Zheng¹, L. Yue¹, Y. F. Lei², M. Xu¹, W. B. Dai^{*1,3}*

¹Hubei Key Laboratory of Plasma Chemistry and Advanced Materials & Key Laboratory of Green Chemical Engineering Process of Ministry of Education, Wuhan Institute of Technology, 430205, Wuhan, P. R. China

²Hubei Key Laboratory of Electronic Manufacturing and Packaging Integration (Wuhan University), Wuhan University, Wuhan, 430072, P. R. China

³Key Laboratory of Testing and Tracing of Rare Earth Products for State Market Regulation, Jiangxi University of Science and Technology, 341000, Ganzhou, P. R. China

**Corresponding author: wubin.dai@wit.edu.cn (W. Dai)*



Scheme S1 The different forms of the assembly modes for the pc-wLEDs, a) traditional packaging via 'the blue LED chip + yellow phosphor YAG: Ce', b) traditional packaging via 'n-UV LED chip + red, green and blue phosphors', c) traditional packaging via 'n-UV LED chip + single-phase white-emitting phosphor', and d) remote 'capping' packaging via 'n-UV LED chip + single-phase white-emitting phosphor', respectively.

Table S1 Instrumental data used for Rietveld refinements for the CYGB host and its Bi/Tb/Eu (co)doped derivatives

Items	Parameters
Primary and second radius	217.5 nm
Receiving slit length	13.65°
Source and sample length	12 mm
Primary slit aperture	2.5°

Reception slit divergence angle	0.2°
Receiving slit width	0.1 mm
Peak-shape function	Lorentzian

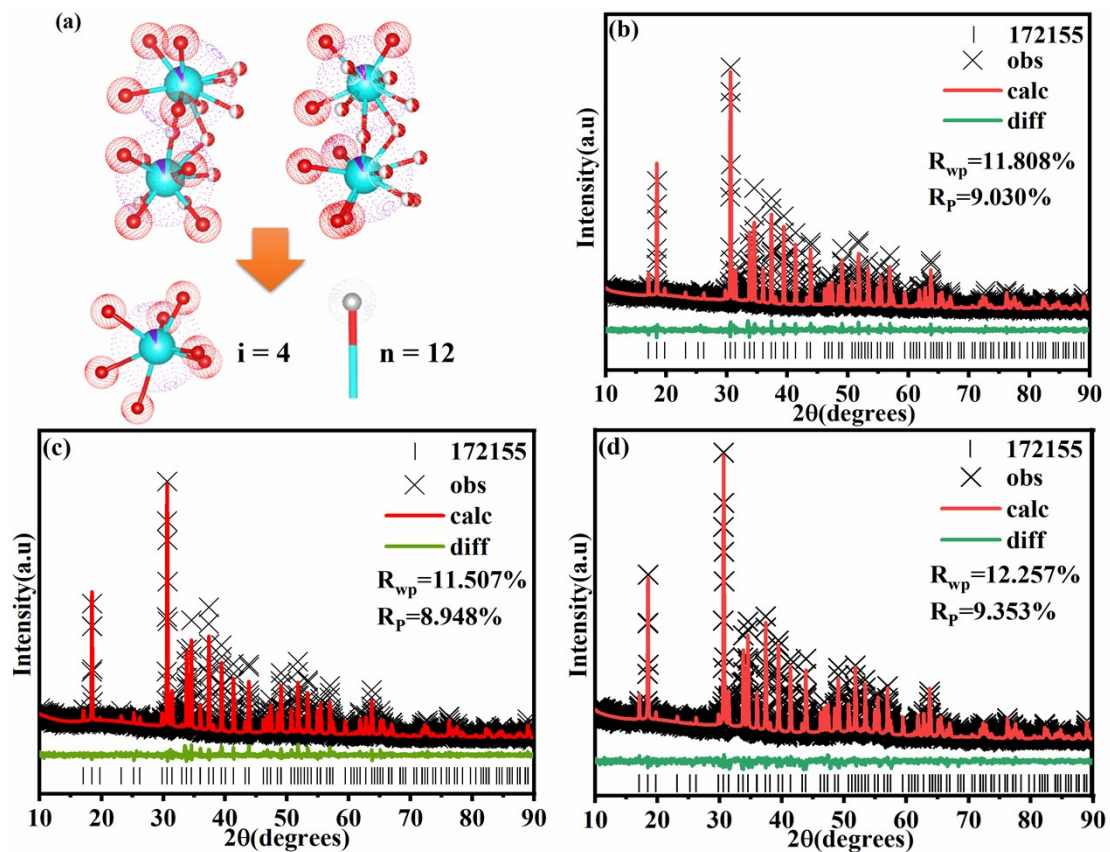


Fig.S1 a) The sketch map for explaining the $CN = 7$ of the Ca_2/Y_2 site in CYGB matrix. The Rietveld refinement results of the sample b) CYGB: 2%Bi, c) CYGB: 2%Bi, 18Tb, and d) CYGB: 10%Tb, 16%Eu, respectively.

Table S2 Selected bond lengths and calculated average bond lengths of the distinct cations Ca_1/Y_1 and Ca_2/Y_2 with surrounding oxygens in CYGB

Vector	Bond length	Average length	Vector	Bond length	Average length
Ca_1/Y_1-O_3	2.47548Å (14)		Ca_2/Y_2-O_4	2.33274Å (9)	
Ca_1/Y_1-O_3	2.47548Å (14)		Ca_2/Y_2-O_4	2.3959Å (3)	
Ca_1/Y_1-O_3	2.47548Å (14)		Ca_2/Y_2-O_4	2.3959Å (3)	

$\text{Ca}_1/\text{Y}_1\text{-O}_3$	2.47548Å (14)		$\text{Ca}_2/\text{Y}_2\text{-O}_4$	2.3959Å (3)	
$\text{Ca}_1/\text{Y}_1\text{-O}_3$	2.47548Å (14)	2.41786Å	$\text{Ca}_2/\text{Y}_2\text{-O}_4$	2.3993Å (3)	2.3955Å
$\text{Ca}_1/\text{Y}_1\text{-O}_3$	2.47548Å (14)		$\text{Ca}_2/\text{Y}_2\text{-O}_4$	2.33274Å (9)	
$\text{Ca}_1/\text{Y}_1\text{-O}_1$	2.3014Å (3)		$\text{Ca}_2/\text{Y}_2\text{-O}_3$	2.41636Å (14)	
$\text{Ca}_1/\text{Y}_1\text{-O}_1$	2.3014Å (3)		$\text{Ca}_2/\text{Y}_2\text{-O}_3$	2.41636Å (14)	
$\text{Ca}_1/\text{Y}_1\text{-O}_1$	2.3014Å (3)		$\text{Ca}_2/\text{Y}_2\text{-O}_2$	2.5043Å (3)	
			$\text{Ca}_2/\text{Y}_2\text{-O}_1$	2.3584Å (3)	

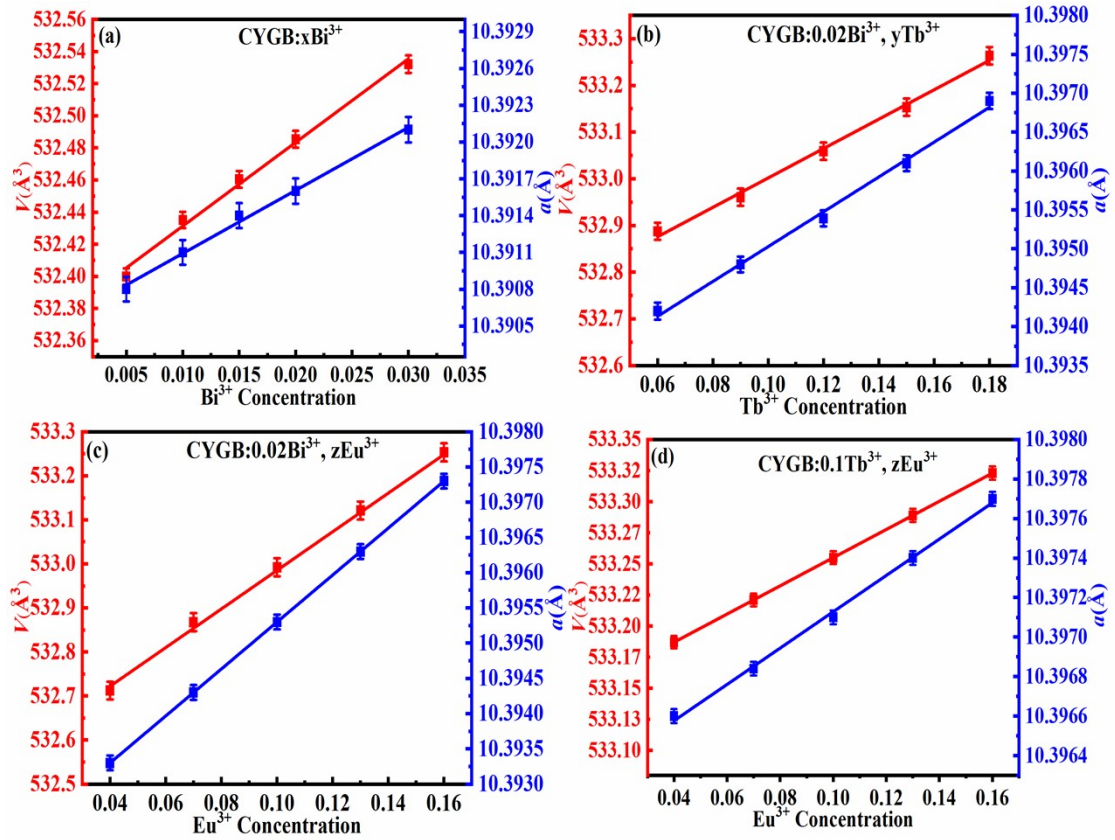


Fig.S2 Lattice parameters of the phosphors a) $\text{CYGB}:x\text{Bi}^{3+}$, b) $\text{CYGB}:2\%\text{Bi}^{3+}, y\text{Tb}^{3+}$, c)

$\text{CYGB}:2\%\text{Bi}^{3+}, z\text{Eu}^{3+}$, and d) $\text{CYGB}:10\%\text{Tb}^{3+}, z\text{Eu}^{3+}$ as a function of x , y , and z as

obtained from the Rietveld refinement of XRD data. All colored solid lines are the linear fits.

Table S3 The weight and atomic percentage of each atom in $\text{Ca}_3\text{Y}(\text{GaO})_3(\text{BO}_3)_4:2\%\text{Bi}^{3+}, 10\%\text{Tb}^{3+}, 12\%\text{Eu}^{3+}$ phosphor

Atom	Weight(%)	Atomic(%)
Ca	16.73	11.54

Y	9.42	2.92
Ga	29.1	11.54
B	6.02	15.39
O	33.4	57.69
Bi	0.58	0.08
Tb	2.21	0.38
Eu	2.54	0.46
Total	100	100

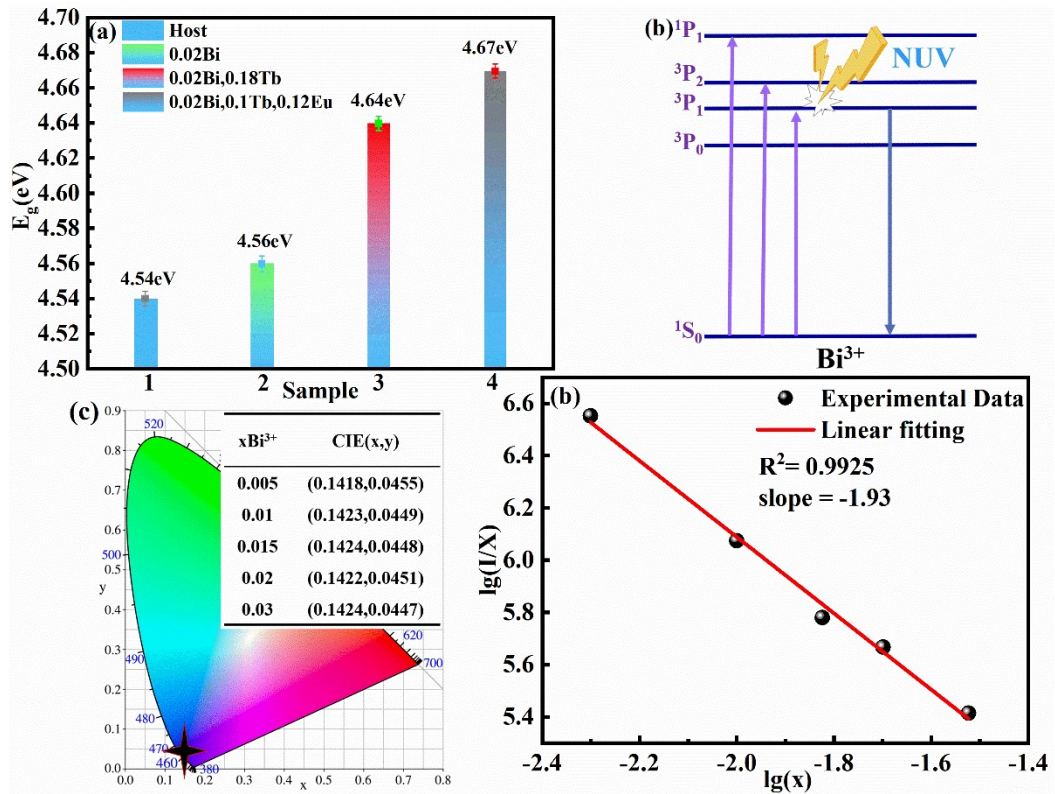


Fig.S3 a) The variation of the bandgap value with the (co)doping content. b) The energy level scheme of the Bi^{3+} ion. c) The CIE diagram for the CYGB: 2%Bi and the CIE coordinates of the phosphors CYGB: $x\text{Bi}^{3+}$. d) The plot of the linear fitting for the $\lg(I/x)$ vs. $\lg(x)$ of the CYGB: 2%Bi.

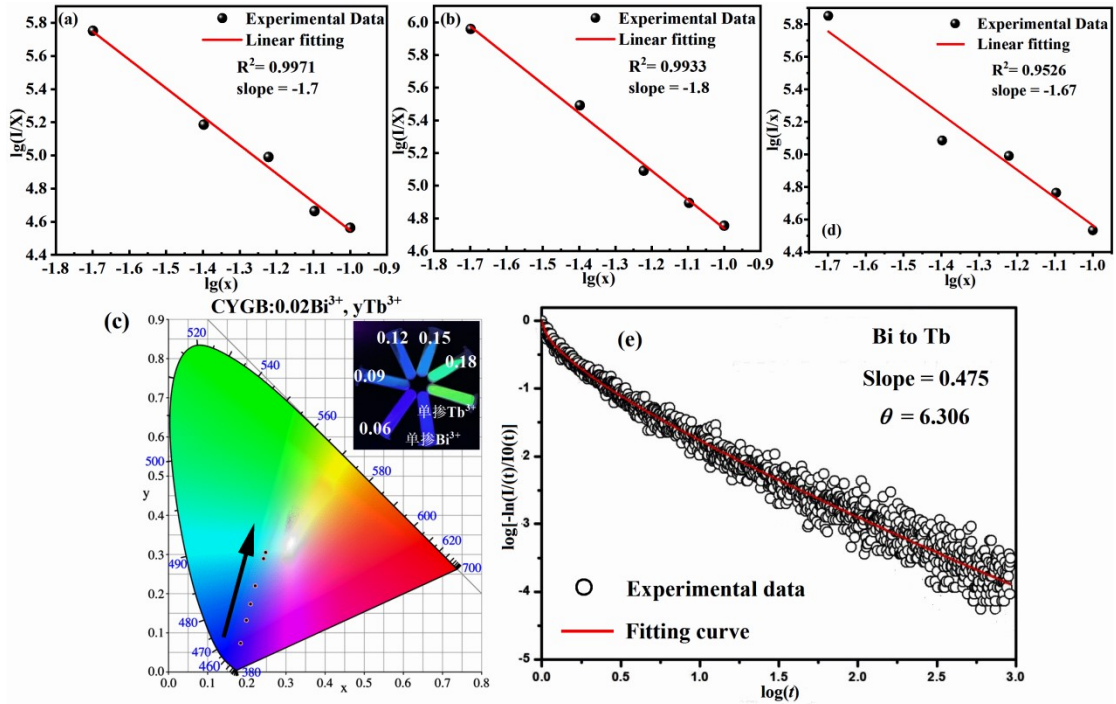


Fig S4 The functional relationship between $\lg(I/x)$ and $\lg(x)$ with their linear fits of the a) CYGB: yTb and b) CYGB: zEu . c) The CIE chromaticity diagram and coordinates of the phosphors CYGB: 2%Bis, yTb , the inset shows the digital images of the phosphors. d) The functional relationship between $\lg(I/x)$ and $\lg(x)$ with its linear fit of the CYGB: 2%Bis, yTb . e) The Inokuti-Hirayama model fitting for the data of the phosphor CYGB: 2%Bis, 18%Tb.

Table S4 The calculated τ_{ave} , ET efficiency (η_{ET}) and probability (P_{ET}) of the representative codoped phosphors *via* fitting the decay curves

	A_1	τ_1 (ns)	A_2	τ_2 (μ s)	τ_{ave} (ns)	η_{ET}	P_{ET}
CYGB: 2%Bis, yTb							
$y = 0$	133	47	352	463.1	446.8	-	-
$y = 9\%$	185	44	328	367.6	327.3	0.267	0.00082
$y = 15\%$	206	43	301	264.1	204.2	0.543	0.0027
$y = 18\%$	247	37	269	142.8	106.4	0.762	0.0072
$y = 21\%$	342	24	186	84.3	69.5	0.844	0.0122
CYGB: 2%Bis, zEu							
$z = 4\%$	146	46	342	376.5	346.2	0.225	0.00065

$z = 10\%$	197	43	316	296.2	263.8	0.409	0.0016
$z = 13\%$	268	39	284	165.9	136.7	0.694	0.0051
$z = 19\%$	351	28	208	126.7	86.4	0.807	0.0093

CYGB: 10%Tb, zEu

$z = 0$	684	7.05 μs	41	1977	1.93 ms	-	-
$z = 4\%$	592	12.06 μs	36	1248	0.53 ms	0.725	1.37
$z = 10\%$	537	10.28 μs	23	895	0.36 ms	0.813	2.26
$z = 13\%$	498	8.42 μs	21	796	0.26 ms	0.865	3.33
$z = 19\%$	461	6.98 μs	18	724	0.24 ms	0.876	3.65

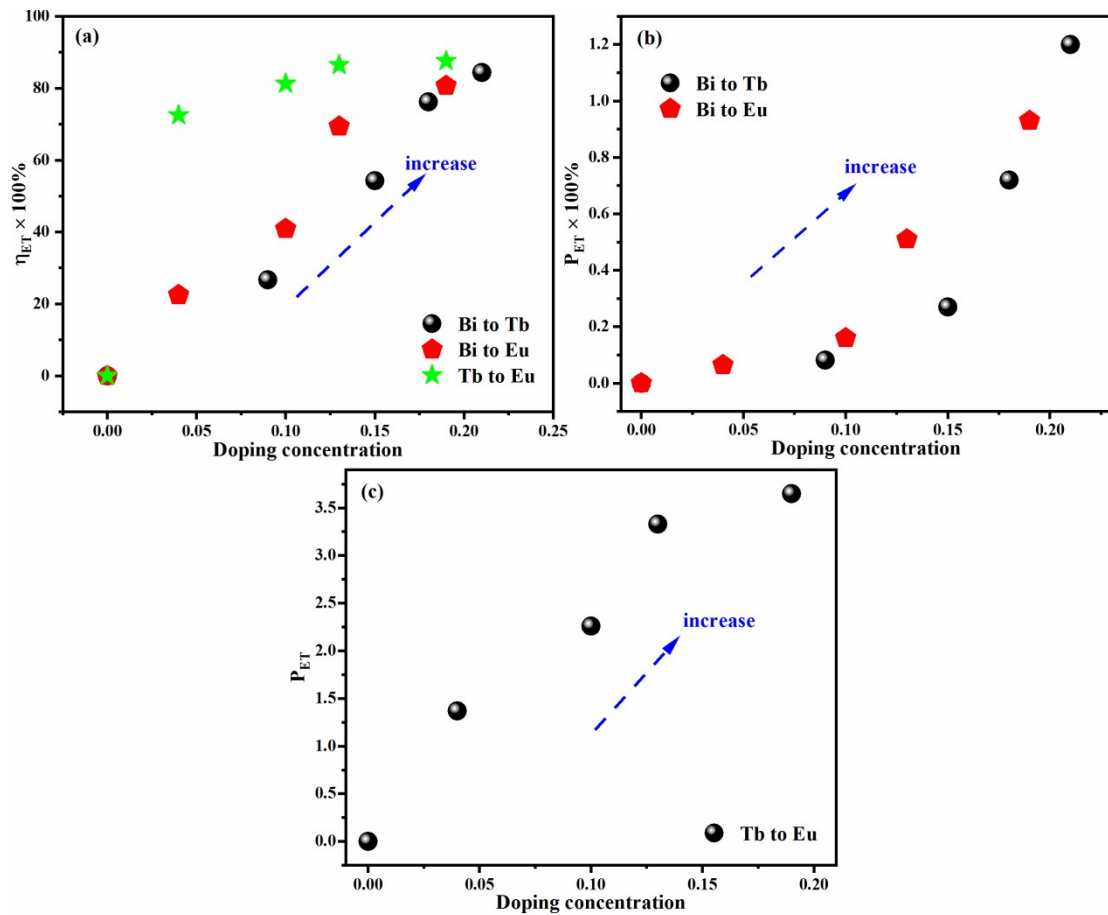


Fig.S5 a) The calculated ET efficiency of the codoped phosphors CYGB: 2%B_i, yTb, CYGB: 2%B_i, zEu and CYGB: 10%Tb, zEu. b) The corresponding ET probability of the codoped phosphors CYGB: 2%B_i, yTb and CYGB: 2%B_i, zEu. c) The corresponding ET probability of the codoped phosphors CYGB: 10%Tb, zEu.

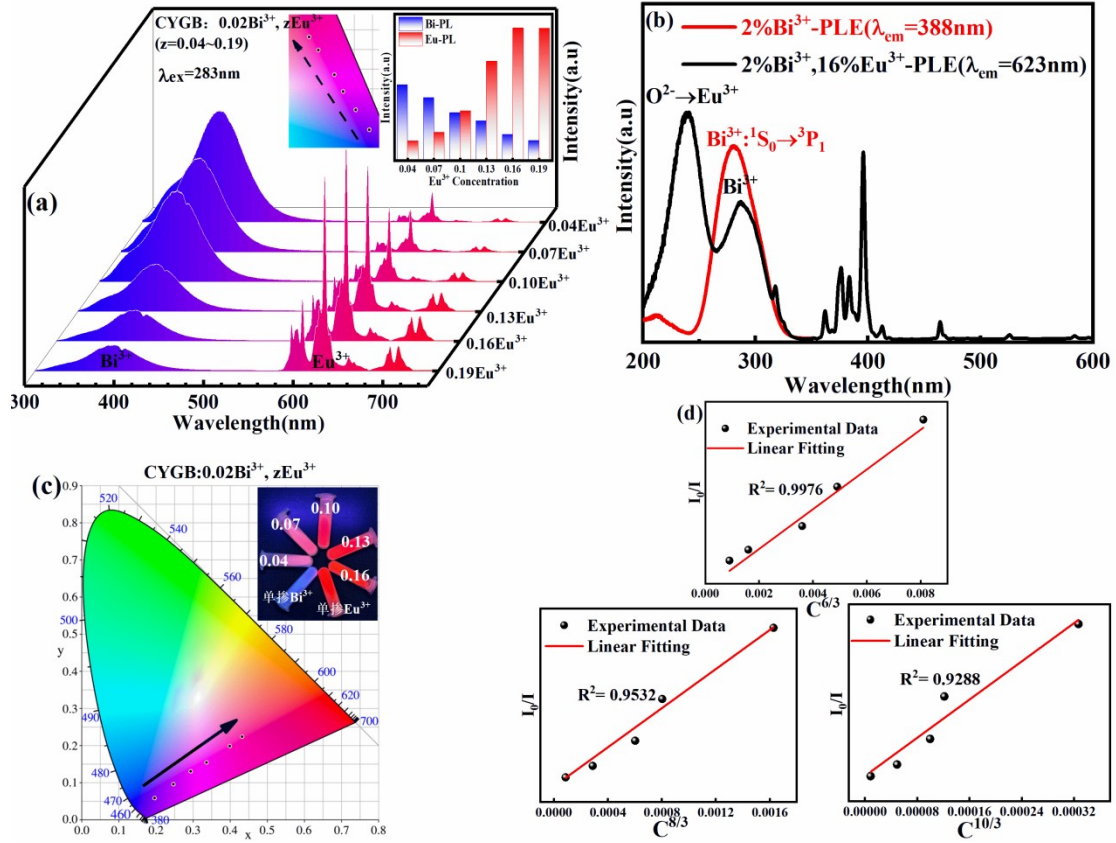


Fig.S6 a) The variation of the PL intensities of the Bi and Eu in the phosphors CYGB: 2%B³⁺, zEu under $\lambda_{ex} = 283$ nm, the insets show the change of the CIE coordinates and the intensity change, respectively. b) The comparison of the PLE spectra of the CYGB: 2%B³⁺ and CYGB: 2%B³⁺, 16Eu under $\lambda_{em} = 388$ nm and $\lambda_{em} = 623$ nm, respectively. c) The variation of the CIE coordinates of the phosphors, the inset shows the corresponding digital image. d) Dependence of I_{S0}/I_S of Bi/Eu on the $C^{6/3}$, $C^{8/3}$ and $C^{10/3}$ in CYGB: CYGB: 2%B³⁺, zEu.

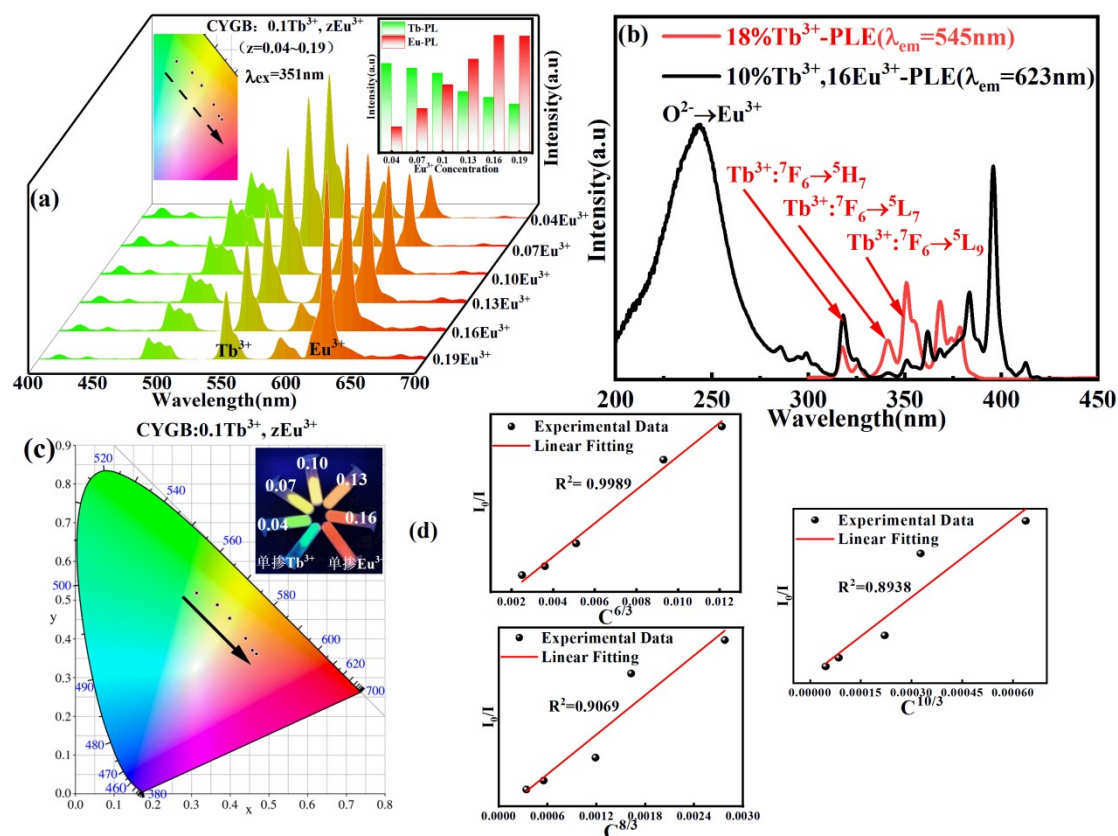


Fig.S7 a) The variation of the PL intensities of the Tb and Eu in the phosphors CYGB: 10%Tb, zEu under $\lambda_{ex} = 351\text{ nm}$, the insets show the change of the CIE coordinates and the intensity change, respectively. b) The comparison of the PLE spectra of the CYGB: 10%Tb and CYGB: 10%Tb, 16Eu under $\lambda_{em} = 545\text{ nm}$ and $\lambda_{em} = 623\text{ nm}$, respectively. c) The variation of the CIE coordinates of the phosphors, the inset shows the corresponding digital image. d) Dependence of I_{S0}/I_S of Tb/Eu on the $C^{6/3}$, $C^{8/3}$ and $C^{10/3}$ in CYGB: 10%Tb, zEu.

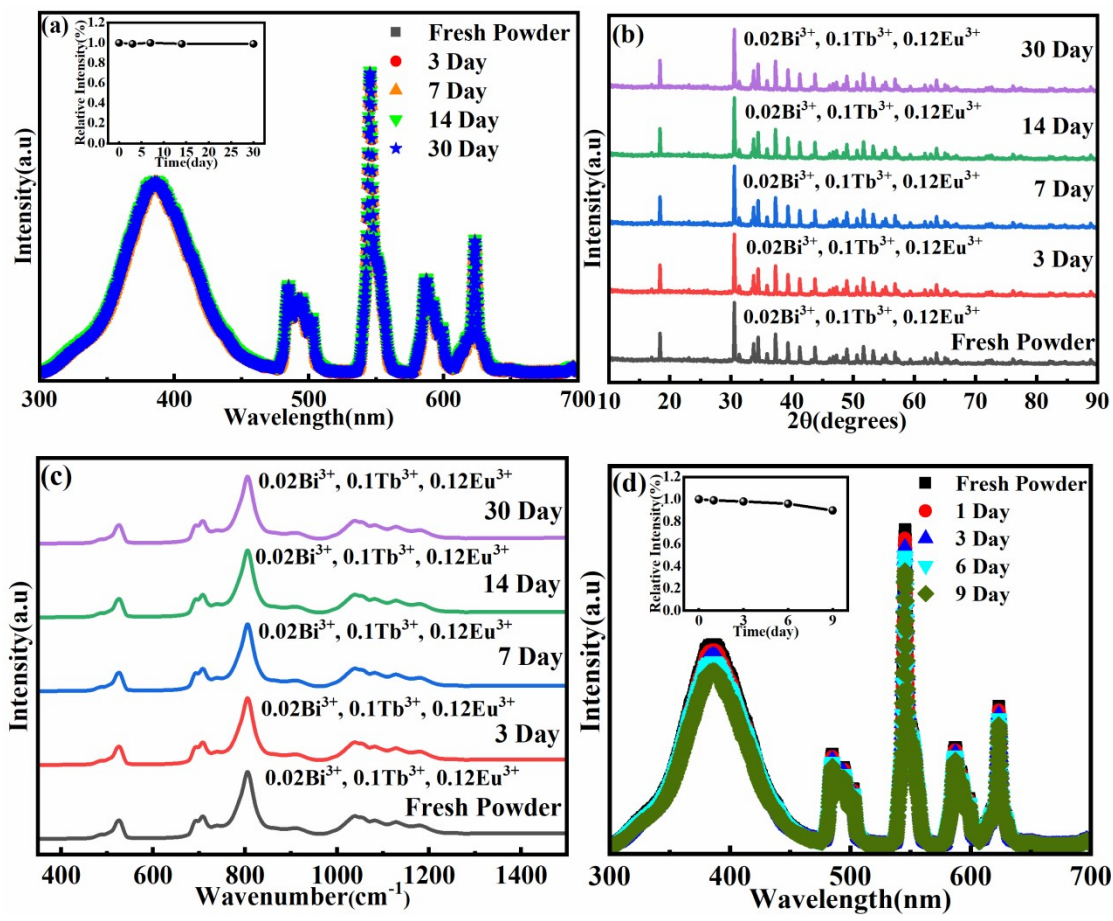


Fig.S8 a) The unchanged PL spectra of CYGB: 2%B_i, 10%T_b, 12%E_u under ambient atmosphere and at RT for different time interval. b-c) The XRD and FTIR spectra of the phosphor before and after one month under exposure to the ambient environment and at RT. d) The slight decrease of the PL intensity of the phosphor CYGB: 2%B_i, 10%T_b, 12%E_u under the harsh conditions (high relative humidity ~ 80% under 323 K) for different time interval, the inset shows the relative PL intensities at measured time.

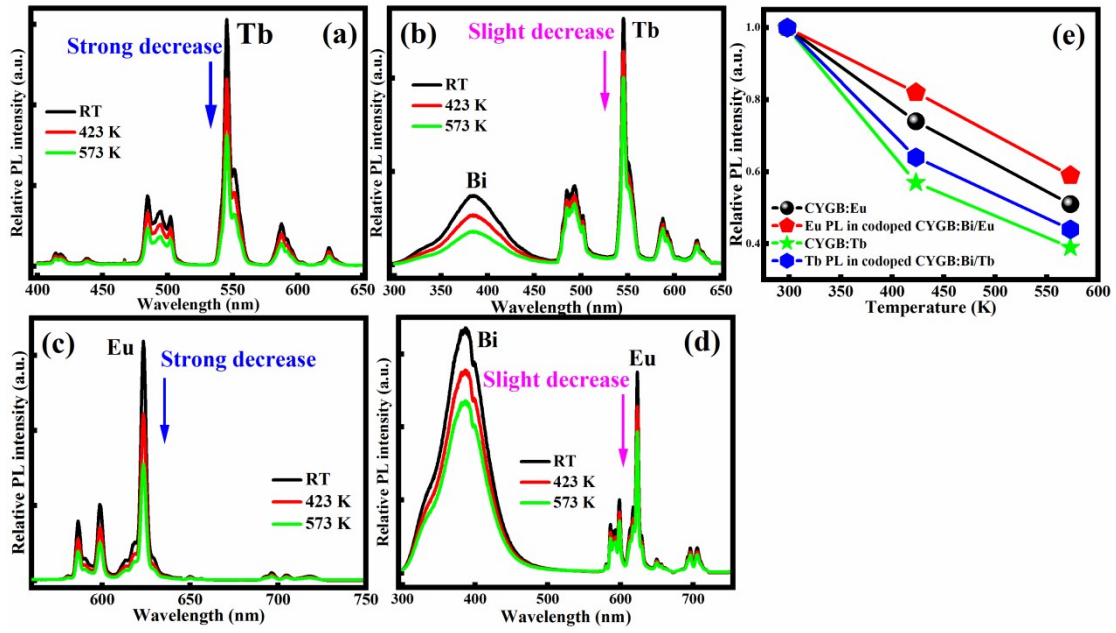


Fig.S9 a, c) The decline of the PL intensities from the Tb and Eu singly doped phosphors CYGB: 10%Tb and CYGB: 12%Eu, respectively under different temperature. b, d) The decrease of the PL intensities of the Tb and Eu in the codoped phosphors CYGB: 2%Bi/10%Tb and CYGB: 2%Bi/12%Eu, respectively under different temperature. e) The comparison of the PL intensities of the Tb and Eu in the singly and codoped phosphors at measured temperature.